International Research Journal of Innovations in Engineering and Technology (IRJIET)

ISSN (online): 2581-3048

Volume 6, Issue 9, pp 18-26, September-2022

https://doi.org/10.47001/IRJIET/2022.609003

Numerical Analysis of the Effect of Free-stream Turbulence on Aerodynamic Performance of NACA 4415 Wind Turbine Airfoil

[1]*Nazaruddin Sinaga, [2]Sukiman

[1]Department of Mechanical Engineering, Faculty of Engineering, Diponegoro University, Jalan Prof. Soedarto, Tembalang, Semarang 50275, Central Jawa, Indonesia

[2]STIMA IMMI, Jalan Raya Tanjung Barat, Jakarta Selatan, Indonesia

*Corresponding Author's E-mail: nsinaga19.undip@gmail.com

***Abstract* - The wind turbine airfoil's aerodynamic performance aerodynamics become essential for the wind turbine. This study aimed to obtain the effect of free-stream turbulence intensity of wind turbine airfoil NACA 4415 using a 2D numerical method. Here, the turbulence intensity varied from 0.1% to 10% at Reynolds number 216,000 and by changing the angle of attack from -4 to 24 degrees, having a chord length of 0.153 m. The finite volume method was used in this study. It was found that the free-stream turbulence intensity can reduce the values of C_D, C_L, C_P, and C_L/C_D but has insignificant effects on the wake area behind the airfoil. The decrease in airfoil efficiency observed was caused by the boundary layer flow disruption, which reduced the total pressure coefficient on the airfoil surface. Likewise, the intensity of turbulence can reduce boundary layer thickness. Finally, the free-stream turbulence controls airfoil performance.**

Keywords: Airfoil, Free-stream turbulence, NACA 4415, Numerical analysis, Wind turbine.

I. INTRODUCTION

The wind is renewable energy currently widely used to generate electricity, replacing non-renewable energy sources. Apart from being more environmentally friendly, the cost of utilizing renewable energy is recently more competitive with fossil energy. Based on Annual Energy Outlook 2019data [1], the cost of producing electricity from coal-fired power plants 4 is 0.12-0.13 USD/kWh, while onshore and offshore wind power, respectively, are 0.037 and 0.106 USD/kWh. The solar cell and thermal power plants are 0.038 and 0.165 USD/kWh, respectively. These costs are based on price-levelized energy costs. It includes the initial capital, investment returns, continuous operation, fuel, maintenance, and time for building a plant with the expected lifetime, as well as capturing carbon and sequestration. It can be seen that for onshore power plants, renewable energy generation costs much cheaper than coal.

One of the wind turbine performance indicators is efficiency or performance coefficient. This indicator is strongly influenced by the design of wind turbines and environmental conditions. Wind speed distribution and turbulence intensity are the critical parameters in designing wind turbine blades[2]. The effect of wind speed on the power and pressure coefficient (C_P) has long been understood. However, the influence of turbulence intensity on these two parameter indicators is still being studied. Wind speed turbulence intensity (TI) is an essential parameter for wind turbines and calculating aerodynamic load.

Renetal. [3] compared the effect of actual turbulence with the Normal Turbulence Model defined by the International Electro technical Commission (IEC) standard. The analysis was conducted based on the available data from onshore wind farms. The results showed that the data supported by IEC overestimated the actual turbulence intensity. Bardal and Saetran[4]studied the impact of turbulence intensity as the wind turbine has a significant role in controlling the power curve and annual energy production (AEP). This way, the calculated AEP becomes 50% less than the standard power curves by considering zero turbulence.

Cao [5] investigated the impacts due to the intensity of turbulence on the performance of asymmetric airfoil S1223 at low Reynolds numbers. The stall of the airfoil becomes delayed while the turbulence intensity increases. Thus, the force of the shedding vortex decreased due to the narrow wake behind the airfoil, suppressing the boundary layer of the airfoil. It was concluded that the TI could increase the generated power of the airfoil. Colman et al. [6]studied the impact of turbulence strength and efficiency of an HQ 17 airfoil. The airfoils were used for two separate turbulent flows with equal mean wind velocity and different turbulence in both the presence and absence of the Gurney Flap, resulting in the output being independent of incoming turbulence. Maldonado et al. [7] examined the impact of free-stream

International Research Journal of Innovations in Engineering and Technology (IRJIET)

ISSN (online): 2581-3048

Volume 6, Issue 9, pp 18-26, September-2022

https://doi.org/10.47001/IRJIET/2022.609003

turbulence on S809 type wind turbine blades with and without turbulent grids, where the turbulence intensity was taken as 6.14%. It was noted that an increase in turbulent intensity could increase the ratio of lift forces to drag forces (C_L/C_D) and delay flow separation at high attack angles.

List of symbols

C_L	:	Lift Coefficient
C_p	:	Pressure coefficient
C_D	:	Drag Coefficient
u	:	Total velocity, m/s
ρ	:	Fluid density, kg/m^3
μ	:	Dynamic viscosity of the fluid, Pa-Sec
ω	:	Angular velocity, rad/sec
ν	:	Molecular kinematic viscosity, Pa-sec
Δy	:	Closest cell distance from the wall, m
U_τ	:	Shear velocity, m/s
$:u'$	:	Fluctuating Velocity, m/s
$\overline{u}$	:	Mean Velocity, m/s

Szehsenyi[8] investigated a turbulent effect on stall conditions on the NACA airfoil profile 634-421. An increase in turbulent intensity could delay stall conditions and increase the upper value of the lift coefficient, thus increasing the resistance of the boundary layer to flow separation. Kim and Xie[9]investigated free-stream turbulence on dynamic stall blades of wind turbines. It was found that the intensity of high turbulence resulted in a reduction in separation bubbles which ultimately increased the ratio of lift to drag coefficient (C_L/C_D) value on static airfoils.

Li et al. [10] performed a direct numerical simulation and experiments for the oncoming stream turbulence strength on the NACA-0012 airfoil. The numerical analysis was matching with the experimental findings. The results achieved by computer simulation were also satisfactory. These results explain that the airfoil stall did not occur at a sufficiently high intensity of turbulence at low turbulence intensity. Moreover, a noticeable impact was observed by the turbulence intensity.

Yao et al. [11] conducted a mathematical analysis using k-ε, RNG k-ε, SST, and Reynolds stress models. They found a similarity between the simulated data and the experimental results. To investigate the calculation accuracy using the computational method, Aftab et al. [12] performed a comparative analysis using several turbulence models for airfoil NACA 4415. According to the turbulence models, the following equations were tested: Spalart-Allmaras (S-A), SST k-ω, (γ) SST, k-kl-ω, and finally, γ-Re SST. In their case, γ-Reθ SST was the preferred model due to a more accurate prediction of flow behavior. However, the difference between the results of calculations with experimental results was still relatively significant. From the above-reported studies, it is concluded that free-stream turbulence is an essential parameter in wind turbine design, and its effect on generating power has not been understood completely. It has both positive and negative impacts on wind turbine performance. Hence, the study on free-stream turbulence demands more analysis to determine its influence on the airfoil.

The present research examined the influence of free-stream turbulence intensity on 2D NACA 4415 airfoil at a Reynolds number of 216.000 using computational fluid dynamics. The study is an initial part of research on the optimum design of wind turbines by considering the free-stream turbulence intensity. These turbulent transition and laminar flows are to be applied to the onshore wind farms in Indonesia. The parameters to be investigated are C_L, C_D, C_L/C_D, $C_{P,}$ and separation positions. Notably, the results are expected to provide a more complete, clear, and precise picture for conducting numerical research on free-stream turbulence intensity in the practical three-dimensional wind turbine of various airfoil types.

II. METHODOLOGY

2.1 Numerical Methods

This study uses the finite volume method to analyze unknown variables by considering nodal points. The Computational Fluid Dynamics (CFD) technique commonly uses Reynolds Average Navier-Stokes (RANS) equations. Here, both mean and fluctuating terms are considered. The total velocity u can be written as a sum of the mean velocity $(\overline{u})$ and fluctuating velocity (u') by the following equation:

$$u = \overline{u} + u' \qquad (1)$$

By considering the instantaneous flow variables, the continuity and momentum equations are as follows:

$$\frac{\partial \rho}{\partial t} + \frac{\partial}{\partial X_i}(\rho u_i) = 0 \qquad (2)$$

$$\frac{\partial}{\partial t}\left(\rho u_i\right)+\frac{\partial}{\partial X_i}\left(\rho u_i u_j\right)=\frac{\partial \rho}{\partial x_i}+\frac{\partial}{\partial x_j}\left[\mu\left(\frac{\partial u_i}{\partial x_j}+\frac{\partial u_j}{\partial x_i}-\frac{2}{3}\delta_{ij}\frac{\partial u_i}{\partial x_i}\right)\right]+\frac{\partial}{\partial x_i}\left(-\rho\overline{u'_i u'_j}\right) \qquad (3)$$

In equation (3), the term $-\rho\overline{u'_i u'_j}$ refers to Reynolds stress, which needs to be modeled.

$$\left(-\rho\overline{u'_i u'_j}\right) = \mu_t\left(\frac{\partial u_i}{\partial x_j}+\frac{\partial u_j}{\partial x_i}\right) - \frac{2}{3}\left(\rho k + \mu_t\frac{\partial u_k}{\partial x_k}\right)\delta_{ij} \qquad (4)$$

International Research Journal of Innovations in Engineering and Technology (IRJIET)

ISSN (online): 2581-3048

Volume 6, Issue 9, pp 18-26, September-2022

https://doi.org/10.47001/IRJIET/2022.609003

2.2 Geometry and Flow Conditions

In this 2D simulation, a NACA 4115 airfoil was used with a chord length of 145 mm, as depicted in Figures 1 and 2. The airfoil is placed in the free air, where the speed and intensity of turbulence and other flow conditions can be regulated. Wall effects experienced in wind tunnel testing are eliminated by using a reasonably extensive calculation domain around the airfoil. The velocity inlet boundary condition is placed on the front and two sides of the airfoil, having a distance of 12 times the airfoil chord length. A pressure outlet boundary condition at the back is the same, including a wall boundary condition. The angle of attack is done by adjusting the direction of speed. In this simulation, the Reynolds number is 216,000 and AOA is varied between -4 and 24 degrees. This study applied free-stream turbulence intensities chosen as 0.1%, 3%, 7% and 10%.

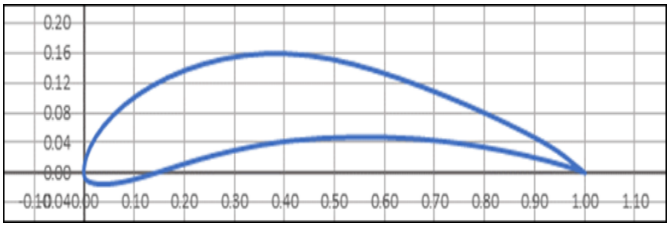

Figure 1: NACA 4415 Airfoil Geometry

2.3 Turbulence Models

The airfoil speed was calculated based on frontal and tangential wind velocity experienced by wind turbine blades. The frontal wind speed of the selected rotor was chosen as 3.4 m/s. This is the designed cut-in speed of the wind propeller available in the laboratory. The rotor speed of the simulation was set to400 RPM so that the tangential velocity at the cut-in speed of the rotor was 22.29 m/s. Thus, the total wind speed at the blade's tip is 22.56 m/s. Using the chord length as the characteristic length and speed, as well as the air properties at atmospheric conditions, the Reynolds number was 216,000. Therefore, the flow regime was considered turbulent with a low Reynolds number.

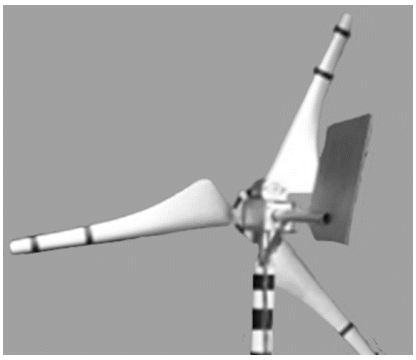

Figure 2: Actual Photograph of Wind Turbine with NACA 4415 Airfoil

The simulation was carried out at a speed of 22.56 m/s calculated based on frontal and tangential wind speeds experienced by wind turbine blades. By using the chord length as the characteristic length and speed, the Reynolds number is 216,000. Therefore the flow regime is turbulent with a low Reynolds number. For such flow conditions, turbulent models that are well used include Spalart-Allmaras and k-ω SST [13, 14]. Based on the argumentation in Mikkelsen [14], the Spalart-Allmaras turbulence model is chosen for this study, which is suitable for the flow with a positive pressure gradient. It does not require wall function, requires relatively few cell numbers, and is more easily converged in a relatively faster time. However, cell size must meet the condition where the value of y^+ (wall distance dimension) must be less than 1. The y^+ value can be estimated from equation (5) below:

$$y^+ = \frac{\rho\, U_\tau\, \Delta y}{\mu} \qquad (5)$$

Where ρ is the fluid density, U_τ is shear velocity, Δy is the closest cell distance from the wall, and μ is the fluid's dynamic viscosity. The transport equation for the modified turbulent viscosity vis :

$$\frac{\partial}{\partial t}(\rho v) + \frac{\partial}{\partial x_i}(\rho v u_i) = G_v + \frac{1}{\sigma_{\tilde{v}}}\left[\frac{\partial}{\partial x_j}\left\{(\mu + \rho v)\frac{\partial v}{\partial x_j}\right\} + Cb2\rho\partial v\partial xj2 - Yv + Sv \right. \qquad (6)$$

Where G_v is the turbulent viscosity for production; Y_v is the turbulent viscosity for destruction; σ_v and C_{b2} refer as constants; ν is the viscosity; S_v is a source term. Notably, the last term has been ignored while estimating the Reynolds stresses.

III. RESULTS AND DISCUSSION

3.1 Grid Independence Test

Based on equation (5) and the size of the calculation domain described above, the number of cells for the first calculation is 62,540. The drag coefficient of the NACA 4415 airfoil is calculated with the number of cells as much as 79,616 and 88,022 and 104,828 and 138,434. These cell numbers are obtained using an adaption method of the cells at the first cell of the boundaries. Based on the criterion of the relative error produced, which is less than 2%, then in this study, the optimal number of cells was selected as 88,202, as shown in Figure 3. The y^+ value for this grid in all simulations is less the 0.25, as seen in Figure 4.

International Research Journal of Innovations in Engineering and Technology (IRJIET)

ISSN (online): 2581-3048

Volume 6, Issue 9, pp 18-26, September-2022

https://doi.org/10.47001/IRJIET/2022.609003

3.2 Selection of Convergence Criteria

This study also tested the convergence criteria for flow and turbulence equations. The residual values tested are 1e-3, 1e-4, and $1e^{-5}$. The test results show that a decrease in the residue will increase accuracy by up to 1%. Nevertheless, in most simulations tested, using a residual of $1e^{-5}$ gives non-convergent results. Therefore, in this study, the convergence criteria for residual errors are $1e^{-5}$.

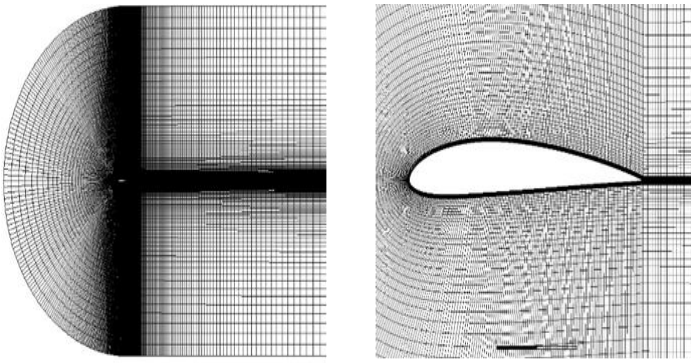

Figure 3: Mesh generation on calculation domain and Near the Airfoil

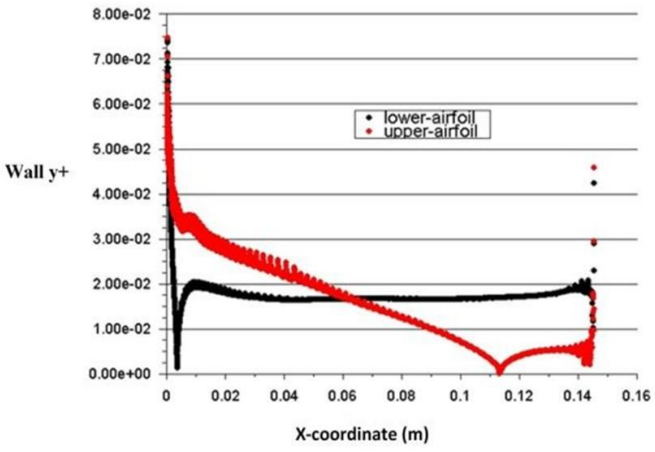

Figure 4: Y^+ Values for Lower and Upper Airfoil

3.3 Validation

In this study, the standard airfoil data of NACA 4115 [12, 13]were used to validate the calculation results. It is necessary to calculate the Reynolds number used, atRe = 3,110,000 and Re = 120,000.

The results of the validation of the C_L values indicate that the calculations gave a fairly good result, with an error of about 12% based on NACA data and 15% for the other one. For AOA = 12 degrees, the validation showed an error of around 8%. Based on these results, it can be said that the calculation of C_L at Re = 216,000 also gave a quite good validation.

3.4 Airfoil performance

3.4.1 Velocity distribution around an airfoil

Figure 5 presents velocity distribution around the airfoil surface at various turbulent intensities. The velocity above the upper surface is higher than the lower surface because of the airfoil camberlength. The flow separates from the upper surface, and the separation intensity grows up with an increase in the angle of attack. The separation point moves forward towards the airfoil leading edge as the angle of attack increases, and this will make the high pressure, which exists on the lower surface, move up to the upper surface.

The lower velocity at a lower surface generates a higher liftforce. At AOA = 0 degree, the effect is not predominant with an increase in TI. However, as turbulent intensity increases, the airfoil's upper surface experiences a higher velocity value than the lower surface. Moreover, near the trailing edge, a massive gap amongst the velocity vectors was observed, explaining the start ofthe flow. At the same time, the stagnation point moves slightly forward at low AOA near the trailing edge.

3.4.2 Pressure distribution around an airfoil

Figure 6 presents the distribution of static pressure around the airfoil surface at turbulent intensities of 0.1-10% for the angle of attack of 0-12°. The contours showed a high pressure at the leading edge (stagnation point), while low pressure manifested at the upper surface. The high-pressure area represents the red color associated with the airflow direction, while blue represents the low-pressure region. The lift force was directed towards Y-axis by pressure difference caused due to the design of the airfoil. Thus, a force was generated, which “pushed” the airfoil upward. While raising the angle of attack, the pressure difference will be augmented by the projected area of the wing, which in turn increases life force, and hence the lift coefficient increases.

3.4.3 Results of C_L and C_D

Figure 7 shows the results of the C_L and C_D for various AOA and turbulence intensities. The reference value was used to calculate the C_D and C_L at a speed of 22.56 m/s with a span area of 0.1453 m^2 and a cross-sectional frontal area of 0.0225 m^2. Figure 7a presents the effect of turbulence intensity, which is relatively straightforward and significant at various AOA. At AOA = 8 to 12 degrees, the impact of TI is to lower the C_L value. The higher the TI, the lower the C_L. The decrease in the CL value is more remarkable at a higher AOA. The gradient of C_L to AOA is getting lower with the increasing value of TI.

International Research Journal of Innovations in Engineering and Technology (IRJIET)

ISSN (online): 2581-3048

Volume 6, Issue 9, pp 18-26, September-2022

https://doi.org/10.47001/IRJIET/2022.609003

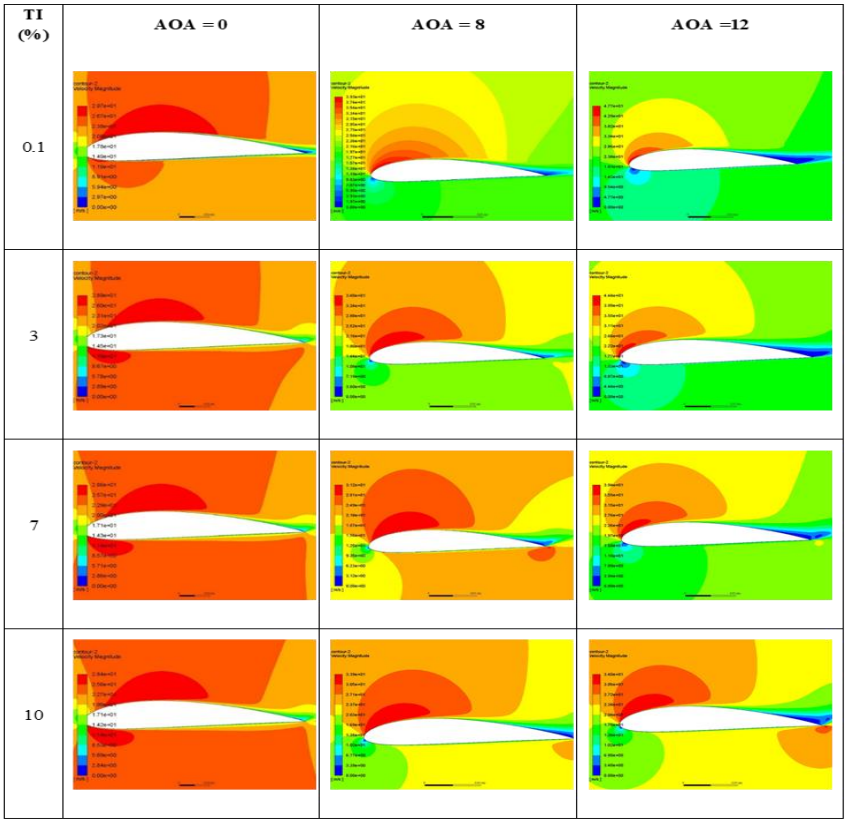

Figure 5: Velocity Contours at Various Values of Angle of Attack and Turbulent Intensity

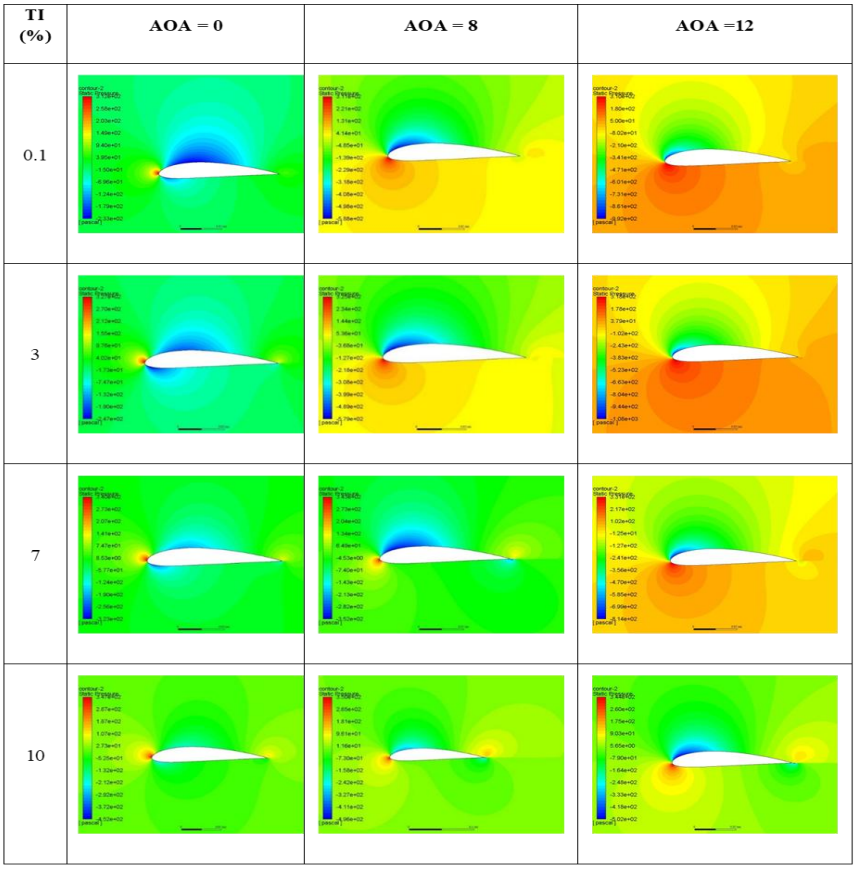

Figure 6: Static Pressure Contours at Various Values of Angle of Attack and Turbulent Intensity

International Research Journal of Innovations in Engineering and Technology (IRJIET)

ISSN (online): 2581-3048

Volume 6, Issue 9, pp 18-26, September-2022

https://doi.org/10.47001/IRJIET/2022.609003

However, the figure also shows that the maximum value of C_L changes to the value of TI. At TI = 7% and 10%, there is an increase in this value, while in TI = 3% degrees, there is a decrease in value. The position of the maximum C_L value also shifts towards the right by increasing turbulence intensity. From Figure 7b, it is clear that the higher the value of TI, the lower the drag coefficient. It certainly positively impacts torque and the power produced by the airfoil. Likewise, the maximum C_D has decreased with the increasing value of TI. The position of the maximum C_D will shift to a larger AOA.

The C_L/C_D can be considered a measure of airfoil efficiency, as shown in Figure 8. At first, the turbulence intensity reduces the distribution of C_L/C_D in almost the entire AOA range. The C_L/C_D tends to decrease with the increased value of TI. The second effect is a shift in the maximum CL/CD value. In this case, if TI increases, the maximum position of C_L/C_D will shift towards a larger AOA. The above results explain a negative effect on free-stream turbulence due to the efficiency of wind turbine airfoils.

3.4.4 Pressure coefficient (Cp)

Figure 9 shows the distribution of pressure coefficients on top and bottom airfoil surfaces, including AOA -8 and 12 degrees at various turbulence intensity. In Figure 9, Cp for the top airfoil lies below the bottom airfoil, indicating that the airfoil has a positive lift or upward force in both AOA values. This follows the CL values distribution in Figure 7a, which shows a positive value. Furthermore, the figure also shows that the distribution of Cp values depends on turbulence.

Increasing the intensity of turbulence will reduce the distribution of C_p values on the upper airfoil, both at AOA = 8 and 12 degrees. However, the distribution of the C_p value also decreases with the increasing value of TI. Since the C_p decrease in the upper part of the bottom is more remarkable, with an increase in the value of TI, the result is a decrease in the value of C_L. This condition applies to AOA = 8 or 12 degrees, but the effect strength is different. At AOA = 8 degrees, the influence of TI is more substantial compared to AOA at 12 degrees. This can be confirmed from the C_L and C_L/C_D values in Figures 7 (a) and 8.

Comparing the results of this study with the previous one is tricky because there are no similar results based on the NACA 4415 airfoil, both experimental and computational. However, the simulation results mentioned above follow a study conducted by Bardal and Saetran[4], which carried out turbine power comparisons that were calculated based on IT assumptions = 0 on power in the field having a high enough turbulence intensity. In these measurements, a power difference of 50% is lower than the power measured by assumptions without turbulence intensity. Likewise, the results obtained by Li et al. [10] on the NACA 0012 symmetry airfoil states that the intensity of turbulence controls the airfoil.

Based on the measurement, Mikkelsen [14] concluded that two effects act oppositely, as observed by free-stream turbulence. Thus, the peak power coincident was reduced by 2.4%, lower than the expected value. Increasing the turbulence enhances the drag on the turbine blades, thus reducing the extraction of power. In the present study, there was a shift in the angle of the stall or angle where the maximum CD occurred, experiencing differences in the turbulence intensity, which is consistent with the results obtained by Maldonado et al. [7], Amandolese and Szechenyi[8], and Li et al. [10].

Mukesh et al. [15] conducted both simulation and experimental work to optimize the airfoil in aerodynamic design. They used a genetic algorithm to perform the simulation and further went on to design the optimized airfoil based on the modeling output. It was shown that the parameters obtained from their experiments closely resemble the simulated data. Earlier, Ghazi and Olwi[16] reported the interference effect of wake turbulence due to a large flapped wing. Although this report does not directly relate to the present study, the researchers showed by numerical analysis that the angle of the trailing wing lifting curves has little to do with wake turbulence.

Abu-Hijleh[17] performed a modeling analysis of isotropic porous floor segments and showed considerable changes in flow filed by changing the porous layers. Daniels et al. [18] performeda numerical analysis to show turbulence's effects on a rectangular cylinder's vortex-induced vibrations. The results showed that the intensity due to turbulence diminished the structural response. Jubran and Hamdan [19] experimented with showing flow velocities' effects on a single cylinder.

In another research, Aarnesa et al. [20] investigated the effects of free-stream turbulence influencing the transition-in-wake state of flow past a cylinder in a circular shape. Wekesa et al. [21] conducted experiments and analyzed turbine turbulence intensity. They showed that the results resemble the aerodynamic behavior. Besides, Ismail and Umukoro [22]conducted several computational analyses on combustion reactions and related emissions to the environment. As is known, the NACA 4415 airfoil is widely used as a wind turbine blade. This airfoil, despite having a low maximum CD value, but its profile has the advantage to use in small Reynolds numbers. The shape of the airfoil profile is quite streamlined so that the boundary layer does not have a bubble having a laminar separation at the front area of the airfoil. Figure 10 shows the separation position that can be estimated from the shear stress distribution in the flow. At AOA = 12 degrees, the separation position can be identified from the

International Research Journal of Innovations in Engineering and Technology (IRJIET)

ISSN (online): 2581-3048

Volume 6, Issue 9, pp 18-26, September-2022

https://doi.org/10.47001/IRJIET/2022.609003

negative value of the shear stress. It appears that the effect of turbulence intensity does not change the separation position much. This follows the simulation results, where the laminar bubble separation phenomenon is not found. Separation occurs near the trailing edge that produces a narrow wake area. Such an airfoil character is not sensitive to the free-stream turbulence intensity. Here, the boundary layer thickness controls the turbulence, which means the higher the intensity of the turbulence, the thinner the boundary layer, decreasing the shearing stress.

Based on the discussion above, it is better to experiment with more precise setups and measuring instruments to do further research on the effects of this turbulence experimentally. Besides, it is necessary to examine the effects of laminar flow, which is influenced by the free-stream turbulence intensity. This research needs to be done given the phenomenon that is still mysterious in the transition area, and there are still various scientific questions about the onset of turbulent flow. The study of numerical methods is also developed further, involving the latest turbulence models. However, the pressure coefficient distribution will decrease, resulting in a higher drop in lifting force coupled with the decline of the frictional force. Finally, C_L/C_D values will decrease, so the airfoil performance will also decrease.

IV. CONCLUSION

Based on the present studies, the first general conclusion is that numerical methods can be used to understand and analyze the flow around the airfoil in detail. Secondly, the free-stream turbulence controls the airfoil, where the impact can increase or decrease the performance. Apart from these, other conclusions can also be presented here. The free-stream turbulence intensity can reduce the values of C_D, C_L, C_P, and C_L/C_D while not significantly affecting the wake area behind the airfoil. The boundary layer flow disruption caused the decrease in airfoil efficiency observed. It reduces the total pressure coefficient. The intensity of turbulence can attenuate the layer thickness. It decreases shear stress.

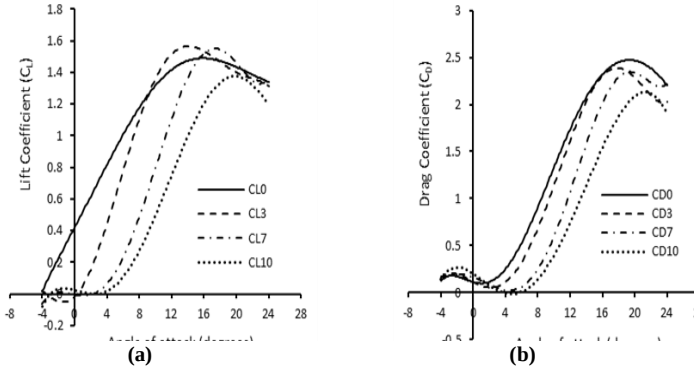

Figure 7: Effect of turbulence intensity on lift and drag coefficient

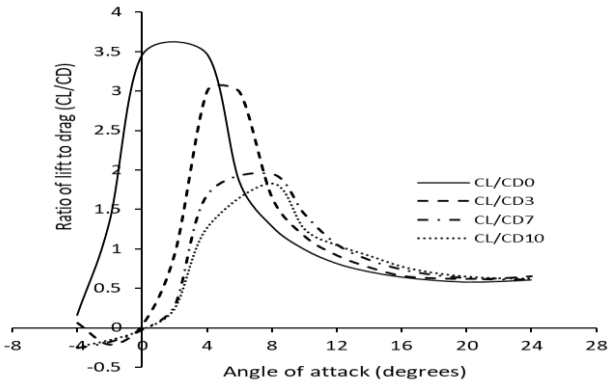

Figure 8: Effect of turbulence intensity on airfoil efficiency (C_L/C_D)

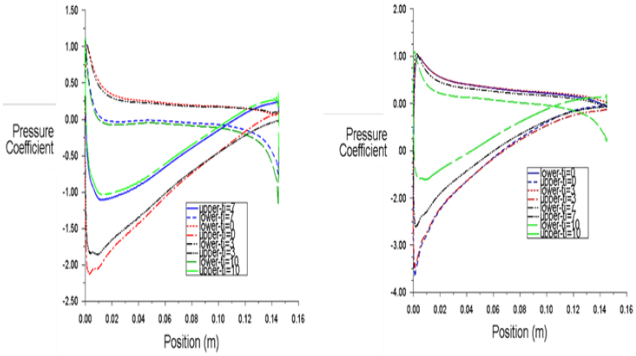

Figure 9: Distribution of C_p on an Airfoil at AOA of (a) 8 degrees (b) and 12 degrees

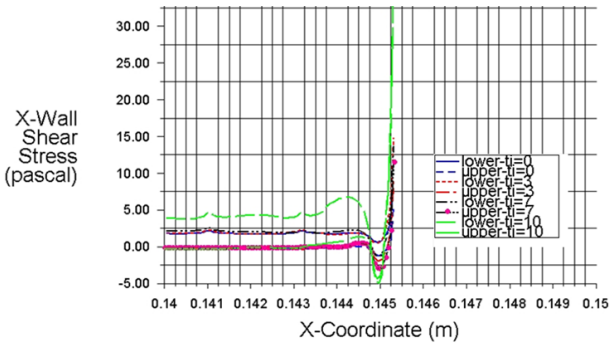

Figure 10: Effect of Turbulence Intensity on Separation Position at AOA = 12 degree

ACKNOWLEDGEMENT

The authors acknowledge the Faculty of Engineering of Diponegoro University for the approved fund that contributed to making the research viable and effective.

CONFLICT OF INTEREST

We confirm that there are no conflicts of interest associated with this publication.

ISSN (online): 2581-3048
Volume 6, Issue 9, pp 18-26, September-2022
https://doi.org/10.47001/IRJIET/2022.609003

REFERENCES

[1] Annual Energy Outlook 2019 with Projection to 2050, U.S. Energy Information Administration, Office of Energy Analysis, U.S. Dept. of Energy, 2019.

[2] Bavin, L.B., Israt, M.I., Harun, C.I., Alam, F., "Effect of turbulence on a Savonius type micro wind turbine," Energy Procedia. 110, 549-554, 2017.

[3] Ren, G., Liu, J., Wan, J., Li, F., Guo, Y., Yu, D., "The analysis of turbulence intensity based on wind speed data in onshore wind farms," Renew. Energy. 123, 756-766, 2018.

[4] Bardal, L.M., Saetran, L.R., "Influence of turbulence intensity on wind turbine power curves," Energy Procedia. 137, 553-558, 2017.

[5] Cao, N., "Effects of turbulence intensity and integral length scale on an asymmetric airfoil at low Reynolds numbers," Thesis submitted to University of Windsor, 2010.

[6] Colman, J., Di, L.J.M., Delnero, J.S., Martínez, M., Boldes, U., Bacchi, F., "Lift and drag coefficients behavior at low Reynolds number in an airfoil with gurney flap submitted to a turbulent flow: Part 1," Lat. Am. Appl. Res., 38, 195-200, 2008.

[7] Maldonado, V., Castillo, L., Thormann, A., Meneveau, C., "The role of free stream turbulence with large integral scale on the aerodynamic performance of an experimental low Reynolds number S809 wind turbine blade," J. Wind Eng. Ind. Aerodyn., 142, 246-257, 2015.

[8] Amandolese, X., Szechenyi, E., "Experimental study of the effect of turbulence on a section model blade oscillating in a stall," Wind Energy, 7, 267-282, 2004.

[9] Kim, Y., Xie, Z.T., "Modelling the effect of free-stream turbulence on dynamic stall of wind turbine blades," Comput. Fluids. 129, 53-66, 2016.

[10] Li, S., Wang, S., Wang, J., Mi, J., "Effect of turbulence intensity on airfoil flow: numerical simulations and experimental measurements," Appl. Math. Mech-Engl., 32, 1029-1038, 2011.

[11] Yao, J., Yuan, W., Wang, J., Xie, J., Zhou, H., Peng, M., Sun, Y., "Numerical simulation of aerodynamic performance for two-dimensional wind turbine airfoils," Procedia Eng., 31, 80-86, 2012.

[12] Aftab, S.M.A, Rafie, A.S.M, Razak, N.A., Ahmad, K.A., "Turbulence model selection for low Reynolds number flows," PLoS One. 11, e0153755, 2016.

[13] Jacob, E.N., Ward, K.E., Pinkerton, R.M., "The characteristics of 78 related airfoil sections from tests in the variable-density wind-tunnel," Report Number 460 National Advisory Committee for Aeronautics (Langley Memorial Aeronautical Laboratory), 1933.

[14] Mikkelsen, K., "Effect of free-stream turbulence on wind turbine performance," Master thesis, Norwegian University of Science and Technology, Department of Energy and Process Engineering, Tornheim, 2013.

[15] Mukesh, R., Lingadurai, K., Selvakumar, U., "Airfoil shape optimization using non-traditional optimization technique and its validation," J. King Saud Univ. - Eng. Sci., 26, 191-197, 2014.

[16] Ghazi, M.A., Olwi, I.A., Interference effects of a large wing on the performance of a trailing wing, J. King Saud Univ. – Eng. Sci., 1, 77-92, 1995.

[17] Abu-Hijleh, B.A.K, "Reattachment of turbulent shear layer over a backwards-facing step with isotropic porous floor segments," J. King Saud Univ. - Eng. Sci., 11, 117-129, 1999.

[18] Daniels, S.J., Castro, I.P., Xie, Z.T., "Numerical analysis of free-stream turbulence effects on the vortex-induced vibrations of a rectangular cylinder," J. Wind Eng. Ind. Aerodyn., 153, 13-25, 2016.

[19] Jubran, B.A., Hamdan, M.N., "Effects of secondary injection on the cross flow-induced vibration of a single cylinder," J. King Saud Univ. - Eng. Sci., 3, 233-248, 1991.

[20] Aarnesa, J.R., Andersson, H.I., Haugen, N.E.L., "Numerical investigation of free-stream turbulence effects on the transition-in-wake state of flow past a circular cylinder," J. Turbul., 19, 252-273, 2018.

[21] Wekesa, D.W., Wang, C.W., Wei, Y., Zhu, W., "Experimental and numerical study of turbulence effect on aerodynamic performance of a small-scale vertical axis wind turbine," J. Wind Eng. Ind. Aerodyn., 157, 1-14, 2016

[22] Ismail, O.S., Umukoro, G.E., "Modelling combustion reactions for gas flaring and its resulting emissions," J. King Saud Univ. – Eng. Sci., 28, 130-140, 2016.

International Research Journal of Innovations in Engineering and Technology (IRJIET)

ISSN (online): 2581-3048

Volume 6, Issue 9, pp 18-26, September-2022

https://doi.org/10.47001/IRJIET/2022.609003

Citation of this Article:

Nazaruddin Sinaga, Sukiman, "Numerical Analysis of the Effect of Free-stream Turbulence on Aerodynamic Performance of NACA 4415 Wind Turbine Airfoil" Published in *International Research Journal of Innovations in Engineering and Technology - IRJIET*, Volume 6, Issue 9, pp 18-26, September 2022. Article DOI https://doi.org/10.47001/IRJIET/2022.609003

****

